Numerical studies of the Anderson transition in three-dimensional quantum site percolation

1996 J. Phys.: Condens. Matter 8 2981

(http://iopscience.iop.org/0953-8984/8/17/010)

J. Phys.: Condens. Matter **8** (1996) 2981–2990. Printed in the UK

Numerical studies of the Anderson transition in three-dimensional quantum site percolation

A W Stadler†, A Kusy† and R Sikora‡

† Department of Electronic Fundamentals, Rzeszow University of Technology, 35-959 Rzeszow, W Pola 2, Poland

‡ Department of Physics, Rzeszow University of Technology, 35-959 Rzeszow, W Pola 2, Poland

Received 12 September 1995, in final form 22 January 1996

Abstract. Numerical studies of the dimensionless conductance g in 3D metal–insulator systems are reported. A site quantum percolation model is defined. It consists of two semi-infinite ideal metal electrodes and a disordered sample of size $L \times L \times L$ located between them. The disorder of the sample is controlled by the metal fraction p of conducting particles randomly occupying the sites of the cubic lattice with probability p. A tight-binding one-electron Hamiltonian with diagonal disorder and a probability density of site energies of the form $P(\varepsilon_n) = p\,\delta(\varepsilon_n) + (1-p)\,\delta(\varepsilon_n - \infty)$ is considered. Magnetic field is also introduced into the model. The conductance g is calculated using the Landauer–Büttiker formula and the Green's function technique. It is found that above the classical percolation threshold—that is, for $p > p_c \simeq 0.312$—a second critical point exists denoted as $p = p_q$. In the region $p_c < p < p_q$, $g \sim \exp(-L/\xi_{loc})$, where ξ_{loc} is the localization length, the system is localized, while in the range where $p > p_q$ the conductance tends to indicate $g \sim L$ metallic-type behaviour. By fitting the estimated data on $\beta(g)$ versus $\ln g$ to the approximate relation for the scaling function β valid in the vicinity of the critical point, the critical conductance is estimated to be $g_c = 1.32 \pm 0.19$ and the correlation length critical exponent is estimated to be $\nu = 1.6 \pm 0.2$. Using a finite-size scaling technique $p_q = 0.44 \pm 0.01$ and $g_c = 1.28 \pm 0.09$ are also found. Both estimates of g_c are expressed in units of e^2/h and are in good agreement with one another. It is found that in the region where $p < p_q$ the system indicates positive magnetoconductance typical for a disorder-induced localized states phase, while in the $p > p_q$ region the magnetoconductance is negative as expected for an extended states phase.

1. Introduction

The evaluation of electrical transport properties of disordered electronic systems has been the subject of a number of theoretical and experimental studies over almost four decades [1]. According to the scaling theory [2] the logarithmic derivative $\beta(g) = \mathrm{d}\ln g/\mathrm{d}\ln L$, which describes the dependence of the dimensionless conductance g on the system size L, is a function of g alone and this function allows one to describe the behaviour of the electronic system when its disorder is varied. In particular, when the dimensionality $d > 2$, $\beta(g) = 0$ separates the extended states (metallic) phase $\beta(g) > 0$ from the localized states phase $\beta(g) < 0$. For $d \leqslant 2$ the wave functions are always exponentially localized, and there is no phase transition in this case. A comprehensive review of electron localization and of the localization transition in the presence of a scattering random potential has been recently given by Kramer and MacKinnon [3]. Other related reviews of this problem including the effects of electron–electron interaction have been given by Lee and Ramakrishnan [4] and, quite recently, by Belitz and Kirkpatrick [5]. The cited reviews may also be considered

0953-8984/96/172981+10$19.50

as a source of further references on numerical studies of the localization transition in the presence of disorder characterized by continuous distributions of site energies.

In numerical studies of disordered electronic systems one often formulates the problem within the framework of a tight-binding Hamiltonian [6–8]:

$$H = \sum_{n} |\boldsymbol{n}\rangle \varepsilon_{\boldsymbol{n}} \langle \boldsymbol{n}| + \sum_{n,m,n\neq m} \exp\left(-\frac{2\pi \mathrm{i}}{\phi_0} \int_{n}^{m} \boldsymbol{A}\ \mathrm{d}\boldsymbol{l}\right) |\boldsymbol{n}\rangle U_{nm} \langle \boldsymbol{m}| \tag{1}$$

where U_{nm} are hopping matrix elements which vanish unless $\boldsymbol{n}$ and $\boldsymbol{m}$ are nearest neighbours, $|\boldsymbol{n}\rangle$ represents a wave function localized near the site $\boldsymbol{n}$, ϕ_0 denotes the unit quantum flux h/e with e and h being the electronic charge and Planck constant respectively, and $\boldsymbol{A}$ is the vector potential of the magnetic field. In the case of the original Anderson localization problem, the site energies ε_n are uniformly distributed over some width which is a measure of the degree of disorder. For quantum percolation systems ε_n is described by a binary distribution which for the site percolation case is [7, 8]

$$P(\varepsilon_n) = p\,\delta(\varepsilon_n - \varepsilon_A) + (1-p)\,\delta(\varepsilon_n - \varepsilon_B) \qquad \varepsilon_A = -\varepsilon_B. \tag{2}$$

Here $\delta = |\varepsilon_A - \varepsilon_B|/zU = 2\varepsilon_A/zU$ determines the degree of disorder, z is the number of nearest neighbours, $U_{nm} = U$ is a constant and p $(1-p)$ is the concentration of sites A (B). Soukoulis *et al* [7, 8] have calculated the mobility edge trajectory, i.e. the line in coordinates p versus the electron Fermi energy E above which the system behaves as a metal (the extended states phase) while it shows insulating behaviour (the localized states phase) below this line. On this basis they found the relation of the quantum percolation threshold p_q to the Fermi energy E for both site and bond percolation problems. Their calculations were performed with the help of the transfer matrix method of MacKinnon and Kramer [9] for varied but finite values of the disorder strength δ. In this method they used long bars of sites having square cross sectional areas of M^2 for which they determined an estimate of the localization length versus M. By increasing M they were able to find the best estimate of localization length for the system studied. This, applied for different values of the concentration p, allowed them to find the mobility edge trajectory. The lowest value of p_q found was $p_q = 0.44 \pm 0.01$, corresponding to $E = 0.5$ measured in units of the transfer energy U. In addition they also calculated the structure of the density of states obtaining a δ-function spike in the centre of the subband $E = \varepsilon_A$ and gap regions on both sides of the central spike in which no states were found. For larger concentrations p no structure (neither a central spike nor a gap) was found in the density of states at around $E = 0$ (i.e. $E = \varepsilon_A$).

In this paper we present results of numerical studies of quantum percolation systems with a site energy distribution which is characteristic of metal–insulator nanocomposites:

$$P(\varepsilon_n) = p\,\delta(\varepsilon_n) + (1-p)\,\delta(\varepsilon_n - \infty) \tag{3}$$

where p $(1-p)$ is probability that a site is occupied by a metallic particle (by the insulator). Thus the site energy randomly takes only the values $\varepsilon_n = 0$ and $\varepsilon_n = \infty$ for the metal and insulator respectively, and the disorder strength $\delta = \infty$.

Our quantum percolation model is addressed to metal–insulator nanocomposites, e.g. RuO_2–glass [10] and granular metal films [6], and it differs by $P(\varepsilon_n)$ given by equation (3) from the previously studied 3D quantum percolation models where $P(\varepsilon_n)$ has the form of equation (2) [7, 8]. The present studies originated from the intention to model the quasi-bicritical transport behaviour of RuO_2–glass films. This behaviour has been inferred from studies of the resistance and $1/f$ noise versus composition as well as resistance versus temperature for different compositions in these films [10, 11, 12]. There

are two important features observed in the above-mentioned experimental dependencies: (i) the temperature coefficient of resistance (TCR) estimated at room temperature changes its sign at a metal concentration lying well above the classical percolation threshold p_c; (ii) in the vicinity of the concentration at which the room temperature TCR changes its sign, $1/f$ noise relative power spectral density strongly increases. These features have been qualitatively described within the framework of the random resistor network with a three-point bond conductance distribution [11]. Such a network indicates two classical transition points: a percolation threshold at p_c and another one at p'_c corresponding to a transition from transport dominated by poorly conducting (but with finite conductance) bonds to transport dominated by well conducting bonds. We think now, however, that in consideration of the electronic transport properties in metal–insulator nanocomposites in which metallic particles are as small as 100 Å, quantum interference phenomena should be taken into account, and, if they are, Anderson localization and an Anderson transition above the classical percolation threshold should take place and in some circumstances may be observed. The resistance versus temperature studies of RuO_2–glass films that we are carrying out at present seem to confirm this suggestion [12].

In this paper we numerically calculate, using the Landauer–Büttiker formula [13] and the Green's function technique [14, 15], the dimensionless conductance versus linear size L of the lattice, concentration p of metallic particles and magnetic field inductance B for an electron Fermi energy $E = 2.0$. We quantitatively estimate and describe the quantum percolation threshold p_q lying at $p_q > p_c$ in our quantum percolation model.

2. Description of the model

We study the quantum site percolation problem on a simple cubic lattice [15]. A fraction p of the sites are occupied by metallic particles and we consider only percolating samples in the regime where $p > p_c \simeq 0.312$, i.e. above the classical percolation threshold. In order to calculate the conductance we connect two opposite walls of a sample of size $L \times L \times L$ with perfect leads, i.e. $p = 1$. We utilize a model of small linear size L ranging from 3 to 8 for the following reasons. The finite-size scaling technique that we apply requires small sample sizes since it works well close to the critical point $\beta(g) = 0$. In particular, the conductance g_c is estimated in this paper from extrapolation of the scaling relations $g(L, p)$ to the point $g(p = p_q, L = 0)$. The magnetic field is applied perpendicularly to one pair of the walls which are not connected to the leads. The Hamiltonian of the quantum percolation model is given by equation (1) with the site energy distribution given by equation (3). The nearest-neighbour hopping matrix element U is taken to be -1 and the electron Fermi energy E is expressed in the units of absolute value of U. The linear size L of the model is measured in units of lattice spacing a assumed as equal to 100 Å, i.e. a typical conducting particle size in RuO_2–glass [10] and granular metal [6] nanocomposites. We follow here the concept of a 2D quantum site percolation model on a square lattice elaborated by Sheng and Zhang [6] to describe Anderson localization in granular metal films that are 2D metal–insulator nanocomposites; 100 Å metallic particles occupy randomly the sites of a square lattice in this model. In our previous paper [15] we presented a 3D extension of the Sheng and Zhang model together with some preliminary results concerning dimensionless conductance and the quantum percolation threshold for an electron Fermi energy $E = 0.01$. As can be seen from the lattice spacing, it is not the original microscopic crystal lattice model. Two nearest-neighbour metallic particles are connected in this model by a short (much shorter than the particle size) confinement or constriction between them. So we can consider here an elementary unit: metallic particle–confinement–metallic particle, which is not like a typical

superlattice system but, rather, like two metallic quantum dots separated by a small and thin cusp of the scattering potential. Transfer of an electron from one metallic particle to the adjacent one is described in our model by the second term of the tight-binding Hamiltonian (equation (1)). The dimensionless conductance of the model is evaluated by using the multichannel Landauer–Büttiker formula [13]:

$$g = \frac{G}{e^2/h} = 4\Big(\sum_{i=1}^{L_0} T_i\Big)\Big(\sum_{i=1}^{L_0} v_i^{-1}\Big)\Big/\Big(\sum_{i=1}^{L_0}(1 + R_i - T_i)v_i^{-1}\Big) \tag{4}$$

where L_0 is the number of quantum channels in the leads, the terms in T_i and R_i are summations of transmission and reflection matrices over L_0, v_i is the channel velocity, and G is the sample conductance. The transmission and reflection matrices have been calculated with the help of the retarded Green's function method. We have chosen equation (4) for calculating the dimensionless conductance since it includes satisfactorily (from the viewpoint of our purpose) the transport properties of the disordered electron system. That is, at each value of the Fermi energy E one finds in this approach the solution for k_x in the following dispersion relation:

$$E/U = 2(\cos k_x a + \cos k_y a + \cos k_z a) \tag{5}$$

where the discrete transverse wave-vector values are $k_y = \pi l/(L+2)$ and $k_z = \pi m/(L+2)$ with l, m taking the values $1, 2, \ldots, L$, i.e. a hard-wall boundary condition is assumed here. Each value k_x^i that is a solution of equation (5) determines one conducting channel with a particular value of the Fermi velocity $v_i = \partial E/\partial k_x$ evaluated at $k_x = k_x^i$. The number L_0 of these conducting channels—that is, the number of values of k_x^i (or v_i)—together with v_i, T_i and R_i, influence the conductance of the system in equation (4). The above-described approach based on the Landauer–Büttiker formula takes into account two parameters, L_0 and v_i, which are not included in some other related numerical techniques. For more details concerning the calculational technique see [14] and [15].

3. Results and discussion

We have performed numerical calculations of the dimensionless conductance g for the above-described quantum percolation model in which disorder was varied by varying the concentration p of occupied sites. These calculations made for different lattice sizes L allowed us to distinguish between the extended states phase and the localized states phase on the basis of the $g \sim L$ and $g \sim \exp(-L/\xi_{loc})$ dependencies which characterize the two phases respectively. ξ_{loc} denotes here the localization length of the electronic wave function. The conductance has been calculated as both a geometric average, $e^{\langle \ln g \rangle}$, and an arithmetic average over 10 000, 5000, 1000, 500, 500 and 500 configurations for $L = 3, 4, 5, 6, 7$ and 8 respectively. In general, the geometric average has been used here to estimate the dimensionless conductance in the localized regime where the self-averaging quantity is $\ln g$ and not g itself. On the other hand, the arithmetic average has been used in the metallic regime where dimensionless conductance appears as the self-averaging quantity.

In figure 1 we show the g versus p relations obtained for the electron Fermi energy $E = 2.0$. We have chosen in this figure the geometric average as an estimate of g in the localized regime and in the metallic regime as well. It is, then, in the metallic regime not the best estimate of g. However, in the metallic regime the geometric and arithmetic averages differ by 22% at $p = 0.45$ and this difference decreases to 2.8% for $p = 0.8$. Since we draw only qualitative conclusions from figure 1 the relations plotted on a logarithmic scale for the conductance are quite satisfactory for such purposes. From this figure one can easily

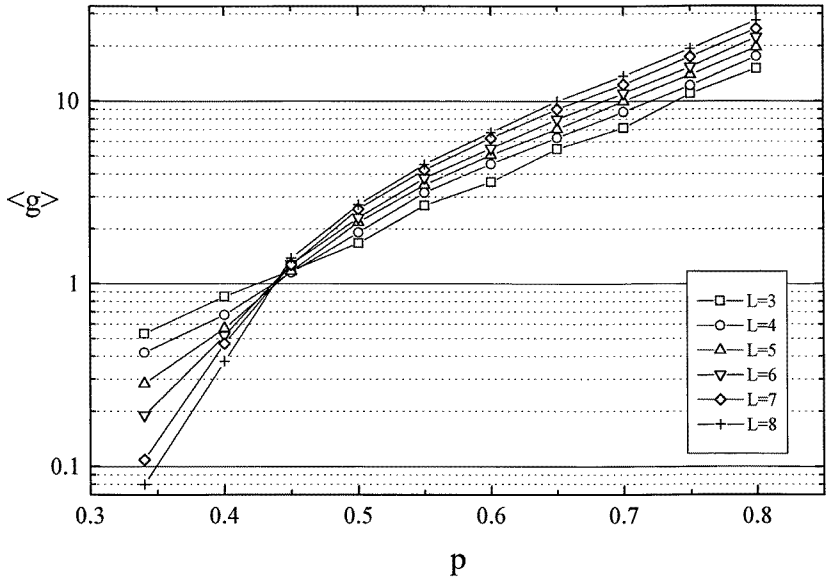

Figure 1. The dimensionless conductance g (equation (4)) of the 3D quantum percolation model versus the concentration p of metallic particles. The geometric average $\langle g\rangle = \mathrm{e}^{\langle \ln g\rangle}$ has been estimated over 10 000, 5000, 1000 configurations for $L = 3, 4, 5$ respectively and 500 configurations for $L = 6, 7, 8$.

see the critical point which may be described by a critical concentration p_q and by a critical conductance g_c in such way that in the range where $p < p_q$ (or equivalently $g < g_c$) the conductance strongly decreases while when $p > p_q$ (or $g > g_c$) it increases with the lattice size L. We have verified the exponential conductance decay and linear conductance increase with L for $p < p_q$ and $p > p_q$ respectively. From figure 1 we roughly estimate $p_q \simeq 0.44$ and $g_c \simeq 1$ in units of e^2/h (see equation (4)) or $g_c \simeq 0.16$ in units of $e^2/\overline{h}$. We will look for p_q- and g_c-values more carefully in the following.

In figure 2 we collect together data points of the scaling function calculated as a numerical logarithmic derivative, using pairs of values for g and L. The set of points presented includes the data shown in figure 1, but in addition we have also included results for $p = 0.41, 0.42, 0.43, 0.44, 0.46, 0.47, 0.48, 0.49$ to increase the number of points in the vicinity of the critical point. The familiar shape of the scaling function $\beta(g)$ [2] can be recognized from the set of results shown. Close to the critical point $\beta(g) = 0$ the approximate formula [16]

$$\beta \equiv \frac{\mathrm{d}\ln g}{\mathrm{d}\ln L} \simeq \frac{1}{\nu}(\ln g - \ln g_c) \tag{6}$$

is fulfilled. Here ν is critical exponent describing divergence of the correlation length ξ

$$\xi \sim \left(\frac{g - g_c}{g_c}\right)^{-\nu} \sim \left(\frac{p - p_q}{p_q}\right)^{-\nu} \tag{7}$$

at the critical point. Below the critical point the correlation length is simply equal to the localization length, ξ_{loc}, while for $g > g_c$ ($p > p_q$) it is such a characteristic length that for $L > \xi$ Ohmic behaviour $g(L) \sim L^{d-2}$ is observed. From equation (6) it is clear that the slope of β versus $\ln g$ as β crosses zero is $1/\nu$. On the basis of this we

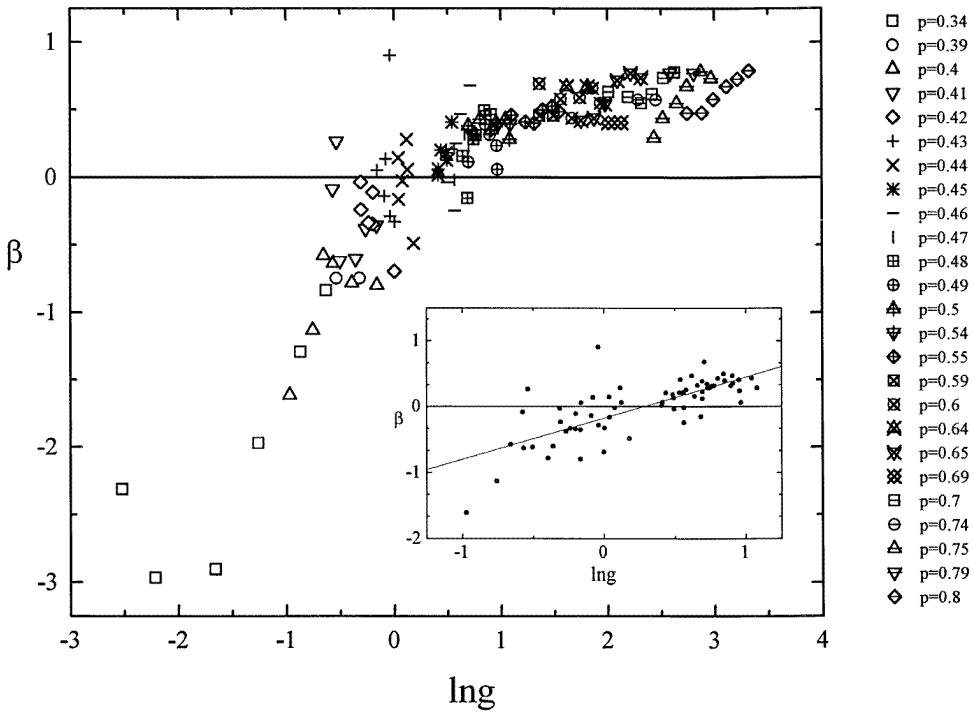

Figure 2. The scaling function β versus the natural logarithm of dimensionless conductance g (equation (4)), estimated as a numerical logarithmic derivative using pairs of values for g and L. The straight line in the inset has been found from the least-squares fit of the numerical results in the range of p bounded to ($p = 0.4$, $p = 0.5$) to the approximate formula (6) expected to hold close to the point $g = g_c$.

have found $\nu = 1.6 \pm 0.2$ and $g_c = 1.32 \pm 0.19$ or $g_c = 0.21 \pm 0.03$ in units of $e^2/\overline{h}$ from the least-squares fit of the straight-line equation to the numerical data bounded to the range ($p = 0.4$, $p = 0.5$). The estimate obtained for ν can be compared with the result $\nu = 1.05 \pm 0.1$ found for metal–insulator transition induced by the magnetic field in diluted magnetic semiconductors below 1 K [17]. The value of $\nu = 0.99 \pm 0.04$ has been extracted from numerical studies of the Anderson model with a Gaussian distribution of site energies [18]. A very recent numerical scaling experiment on the Anderson model with a uniform distribution of site energies based on the Kubo–Greenwood expression has led, however, to the value of $\nu = 1.5 \pm 0.2$ [16]. The same value (in fact, $\nu = 1.5 \pm 0.1$) has been published by Kramer and MacKinnon [3]. We have to point out here that our results for ν have been found for one particular value of the Fermi energy, $E = 2.0$.

To test quantitatively how the dimensionless conductance g depends on the lattice size L we have plotted g versus L for different metallic particle concentrations (figure 3). In the range where $p < p_q$ (figure 3(a)), the scale of g is logarithmic and straight-line relationships of the form $\ln g \sim -L/\xi_{loc}$ have been verified for different p-values. In particular, one can see that the magnitude of the straight-line slope decreases continuously to zero as p approaches p_q; thus $\xi_{loc} \to \infty$ with $p \to p_q$ is observed. On the basis of this we can, with more confidence than from figure 1, estimate $p_q^- = 0.44$ as the highest metal concentration for which a negative slope is still observed. For $p = 0.45$ a positive slope

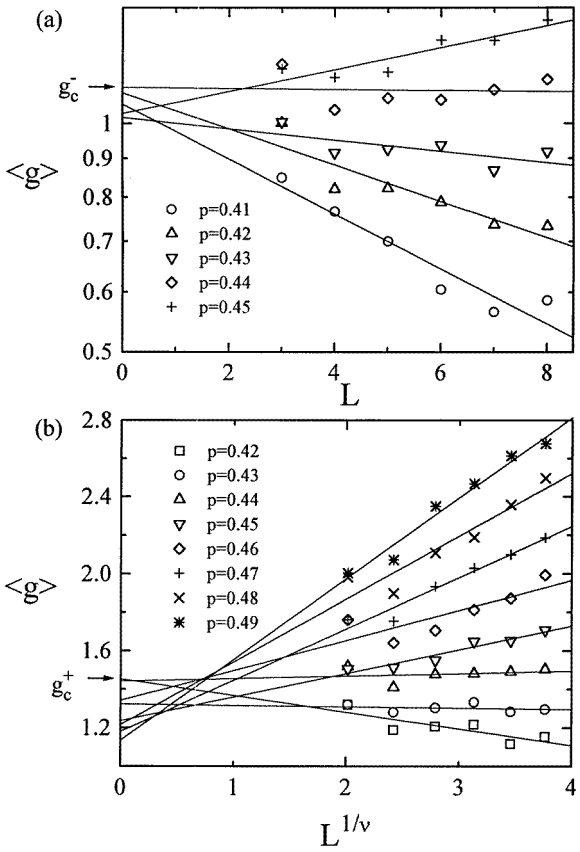

Figure 3. The dimensionless conductance g versus the linear size of the 3D quantum percolation model for different concentrations p of occupied sites. (a) Verification of the scaling formula $g = g_c \exp(-L/\xi_{loc})$ in the range where $p < p_q$ and an estimation of g_c from the intersection of the straight line with the negative slope of smallest magnitude with the g axis, $g_c^- = g(p = 0.44, L = 0)$; $\langle g \rangle$ denotes the geometric average of g over 10 000, 5000 configurations for $L = 3, 4$ respectively and 2000 configurations for $L = 5, 6, 7, 8$. (b) Verification of the scaling formula $g = g_c + \gamma(L/\xi)^{1/\nu}$ in the range where $p > p_q$ and an estimation of g_c from the intersection of the straight line having the positive slope of smallest magnitude with the g axis, $g_c^+ = g(p = 0.44, L = 0)$; $\langle g \rangle$ denotes the arithmetic average over the same number of configurations as in (a); $\nu \simeq 1.6 \pm 0.2$ found in this work has been used for the $L^{1/\nu}$ axis. For $L = 3$, variation of p with the step 0.01 does not result in any change of g.

of the straight line first appears. We can also estimate g_c with the help of the relation $g = g_c \exp(-L/\xi_{loc})$ which is expected to hold slightly below the critical point. With a logarithmic scale for g we find g_c as the intersection of the straight line having the negative slope of the smallest magnitude with the g axis: $g_c^- = g(p_q = 0.44, L = 0)$. On this basis we find $g_c^- = 1.12 \pm 0.09$ or, in units of $e^2/\hbar$, $g_c^- = 0.178 \pm 0.014$, which is in good agreement with $g_c = 1.32 \pm 0.19$ ($g_c = 0.21 \pm 0.03$ in units of $e^2/\hbar$) found from β versus $\ln g$ at $\beta = 0$ (equation (6)).

On the other side of the critical point, for $p > p_q$ (figure 3(b)) one expects, far above p_q, a linear relationship for g versus L. Close to p_q, however, finite-size scaling shows [16] that the conductance should scale as $g = g_c + \gamma(L/\xi)^{1/\nu}$ where γ is a constant. On the basis

of our estimate of $\nu = 1.6 \pm 0.2$ found from β versus $\ln g$ (figure 2) we have plotted g versus $L^{1/\nu} \simeq L^{0.625}$ for p in the range 0.42–0.49. A linear conductance scale and an arithmetic average have been used in this case. As can be seen, the results plotted in such coordinates can be fitted to the straight lines with a slope which decreases as p decreases from $p = 0.50$ down to 0.44. For $p = 0.44$ we observe a very small but positive slope, while for $p = 0.43$ the slope starts to be negative, also with a very small magnitude. Thus we estimate here $p_q^+ = 0.44$ which is equal to p_q^-. By extrapolating the straight line for $p = 0.44$ to $L = 0$ we find from the intersection with the g axis $g_c^+ = g(p = 0.44, L = 0) = 1.44 \pm 0.09$ (or $g_c^+ = 0.230 \pm 0.014$ in units of $e^2/\hbar$). The two procedures of approaching the critical point from below and from above allow us to estimate the quantum percolation threshold value as $p_q = 0.44 \pm 0.01$. We estimate g_c as the arithmetic average of g_c^- and g_c^+; thus $g_c = 1.28 \pm 0.09$ or $g_c = 0.21 \pm 0.02$ in units of $e^2/\hbar$. The value obtained here for p_q can only be compared with $p_q \simeq 0.45$ found by Soukoulis *et al* [8] for the same Fermi energy $E = 2.0$ and site energy distribution given by equation (2). When dealing with the estimate obtained for g_c we compare in units of $e^2/\hbar$ our value $g_c = 0.21 \pm 0.02$ with $g_c = 0.10 \pm 0.01$ found from numerical scaling experiments based on the Anderson model with a uniform distribution of site energies and the Kubo–Greenwood expression for the conductivity [16]. The most commonly reported value of g_c in units of $e^2/\hbar$ is usually in the range 0.03–0.2; however, values of g_c as large as 1 and 10 have also been found [19].

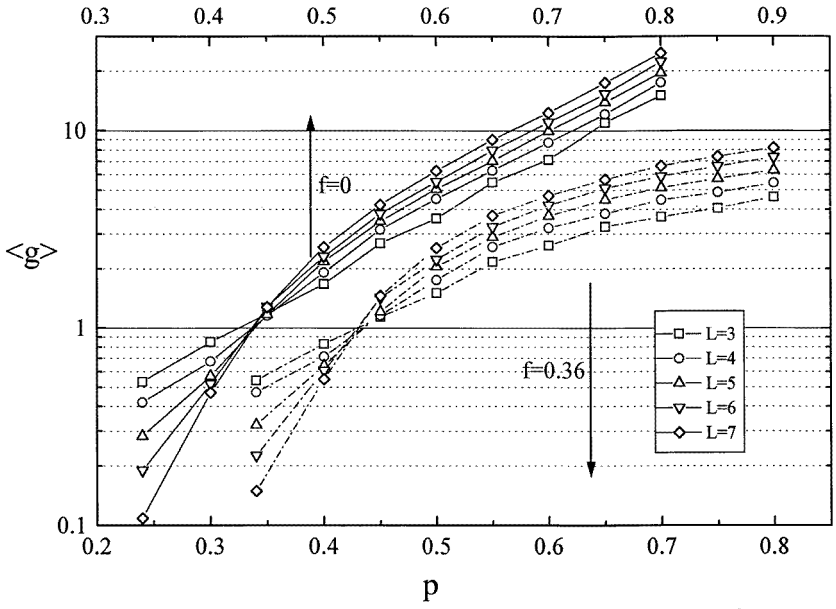

Figure 4. The results up to $L = 7$ repeated from figure 1 and, in addition, data of the same type but with the application of an external magnetic field (perpendicular to one pair of the walls without electrodes) for the strength characterized by the value $f = 0.36$ of the quantum flux fraction $f = Ba^2/\phi_0$ which with $a = 100$ Å typical for metal–insulator nanocomposites corresponds to $B = 15$ T. The normal negative metallic magnetoconductance for $p > p_q$ and positive localization magnetoconductance for $p < p_q$ can be clearly seen.

In figure 4 we show the numerically evaluated g versus p relations with the magnetic field applied perpendicularly to one pair of the walls to which current feeding electrodes are not connected. The strength of the magnetic field is characterized by the fraction of

quantum flux, $f = Ba^2/\phi_0$. The value $f = 0.36$ used to obtain the data shown in figure 4 corresponds to $B = 15$ T for the assumed value of $a = 100$ Å typical for metal–insulator nanocomposites [6, 10]. As can be seen from figure 4 the magnetic field slightly decreases the quantum percolation threshold from $p_q \simeq 0.44$ for $f = 0$ to $p_q \simeq 0.43$ for $f = 0.36$ and the critical conductance, respectively, from $g_c \simeq 1.3$ to $g_c \simeq 1.0$. Since the applied magnetic field is relatively strong (and for smaller fields an even smaller influence has been found) we see that magnetic field only slightly changes the coordinates of the critical point. In the extended states phase the magnetic field generally decreases the dimensionless conductance. This decrease is hardly seen close to the critical point, and the greater the distance from p_q the greater the magnitude of the conductance attenuation. Thus the magnetoconductance is negative for $p > p_q$ and its magnitude decreases evidently with the increase of the metal concentration. This is known behaviour, described by $\Delta G/G \simeq (\omega_c\tau)^2$, where G is the conductance, ΔG is its change under a magnetic field, ω_c is the electronic cyclotron frequency and τ is the elastic scattering time [20]. Quite opposite is the behaviour of the conductance in the localized states phase. g slightly increases for this phase with magnetic field. This is consistent with the picture of electron wave localization. The magnetic field breaks down the time-reversal invariance of the medium. Therefore with an externally applied magnetic field, the coherent backscattering effect is reduced, which implies an increase in the conductivity. The positive magnetoconductance is an inherent characteristic of the disorder-induced localized states phase. This is a qualitative description of the observation concluded on the basis of the influence of the magnetic field shown in figure 4. It reveals, however, the very interesting methods of numerical study that can be carried out using the technique described here for the disordered electronic system with an applied external magnetic field.

4. Concluding remarks

To summarize, it has been shown in this paper that using a model of a 3D mesoscopic granular metal system and the Landauer–Büttiker formula together with the retarded Green's function technique one can obtain a clear signature of the Anderson transition. Because of the high electron density in the metal, neglect of electron–electron correlation may be justified. The scattering strength has been controlled by the concentration p of the metal, which can be easily realized in metal–insulator nanocomposites. The idea of such numerical studies as a tool for prediction of localization behaviour of 2D granular metal nanocomposites was first suggested by Sheng and Zhang [6]. In this paper we have presented an extension of this idea to 3D mesoscopic metal–insulator systems. Using a lattice of relatively small linear size L and a finite-size scaling technique, appropriate for such small sizes close to the critical point for Anderson transition, we have shown that a 3D metal–insulator nanocomposite indicates, above the classical percolation transition, characterized by the critical concentration $p_c \simeq 0.312$, also a quantum percolation transition characterized by the critical concentration p_q, which for one particular electron Fermi energy $E = 2.0$ is $p_q = 0.44 \pm 0.1$. In addition, the transition point has also been characterized by a critical conductance $g_c = g(p_q) = 1.28 \pm 0.09$ in units of e^2/h or $g_c = 0.21 \pm 0.02$ in units of $e^2/\hbar$. The correlation length critical exponent found from the behaviour of the $\beta(g)$ scaling function as $\nu = 1.6 \pm 0.02$ remains in rough agreement with most recent estimates of this exponent [3, 16].

The bicritical behaviour observed here may be used to model the electrical transport behaviour of RuO_2–glass films [10, 11, 12] or other metal–insulator nanocomposites. In such systems experimental identification of the classical percolation transition and the

quantum percolation transition may be difficult when the two transition points lie close to the concentration (p) axis. Our earlier experimental studies based on the temperature characteristic of resistance and $1/f$ noise behaviour, both versus the concentration of the metallic component in RuO_2–glass nanocomposites [10, 11, 12], seem to indicate that the model presented in this paper may be of some use in the interpretation of the observed low-temperature (below 1 K) and room temperature characteristics.

Acknowledgments

Fruitful discussions with N Giordano and T Dietl are gratefully acknowledged. This work was supported by the State Committee of Scientific Research (KBN), grant No 8 T11 B 038 09.

References

[1] Anderson P W 1958 *Phys. Rev.* **100** 1492
[2] Abrahams E, Anderson P W, Licciardello D C and Ramakrishnan T V 1979 *Phys. Rev. Lett.* **42** 673
[3] Kramer B and MacKinnon A 1993 *Rep. Prog. Phys.* **56** 1496
[4] Lee P A and Ramakrishnan T V 1985 *Rev. Mod. Phys.* **57** 287
[5] Belitz D and Kirkpatrick T R 1994 *Rev. Mod. Phys.* **66** 261
[6] Sheng P and Zhang Z Q 1991 *J. Phys.: Condens. Matter* **3** 4257
Zhang Z Q and Sheng P 1991 *Phys. Rev.* B **44** 3304
[7] Soukoulis C M, Economou E N and Grest G S 1987 *Phys. Rev.* B **36** 8649
[8] Soukoulis C M, Li Q and Grest G S 1992 *Phys. Rev.* B **45** 7724
[9] MacKinnon A and Kramer B 1983 *Z. Phys.* B **53** 1
[10] Bobran K and Kusy A 1991 *J. Phys.: Condens. Matter* **3** 7015
[11] Kusy A and Listkiewicz E 1988 *Solid State Electron.* **31** 821
Kusy A and Kolek A 1989 *Physica* A **157** 130
Kolek A and Kusy A *Phys. Rev.* B **43** 11 274
[12] Kusy A 1996 in preparation
[13] Büttiker M, Imry Y, Landauer R and Pinhas S 1985 *Phys. Rev.* B **31** 6207
[14] McLennan M J, Lee Y and Datta S 1991 *Phys. Rev.* B **43** 13 846
[15] Kusy A, Sikora R and Stadler A W 1994 *Physica* A **211** 381
[16] Lambrianides P and Shore H B 1994 *Phys. Rev.* B **50** 7268
[17] Jaroszynski J and Dietl T 1992 *Physica* B **177** 469
[18] Chang T M, Bauer J D and Skinner J L 1990 *J. Chem. Phys.* **93** 8973
[19] Kaveh M and Mott N F 1987 *Phil. Mag.* B **55** 9
[20] Kittel C 1970 *Introduction to Solid State Physics* (New York: Wiley) Polish edition, p 252